Anal. Bioanal. Electrochem., Vol. 11, No. 5, 2019, 625-634

Analytical &
Bioanalytical
Electrochemistry

2019 by CEE
www.abechem.com

Full Paper

Facile Electrosynthesis of Zinc-doped Superparamagnetic Iron Oxide Nanoparticles and their Surface Capping with Dextran Layer for Biomedical Uses

Ali Ahmadi*

Materials and Nuclear Research School, Nuclear Science and Technology Research Institute (NSTRI), P.O. Box 14395-834, Tehran, Iran

*Corresponding Author,

E-Mail: aahmadi@aeoi.org.ir

Received: 20 January 2019 / Received in revised form: 17 April 2019 / Accepted: 28 April 2019 / Published online: 31 May 2019

Abstract- In this study, superparamagnetic iron oxide nanoparticles (SPIONs) are simply fabricated through a one-step electrodeposition method, and their *in situ* surface capping with dextran layer and crystal structure doping with zinc cations are simultaneously performed during their electrochemical synthesis. A simple conditions of room temperature, two-electrode electroplating, direct current synthesis and pH=6.7 were applied in the electrodeposition process. The fabricated SPIONs are characterized through Fourier transform infrared (FTIR) spectroscopy, X-ray powder diffraction (XRD), field-emission scanning electron microscopy (FE-SEM), vibrating sample manometer (VSM), thermogravimetric (TG) and differential scanning calorimetry (DSC) analyses. These analyses results indicated that the prepared SPIONs have particles with 15nm size. The magnetic characters i.e. saturation magnetization (*Ms*), remanence (*Mr*) and coercivity (*Hci*) values of the fabricated SPIONs were measured to be 51.75 emu g^{-1}, 0.16 emu g^{-1} and 3.35 Oe, respectively. It was found that the dextran surface capped-, zinc doped- SPIONs are proper candidates for biomedical investigations.

Keywords - Magnetic oxide, Structure doping, Nanoparticles, Electrochemical synthesis, Surface capping, Biomedical

1. INTRODUCTION

In recent decade, considerable investigations have been carried out in the development of superparamagnetic iron oxide nanoparticles (SPIONs), improving their magnetic characters, and maximizing their applicability in many various biomedical areas [1-5]. Precise control over the fabrication parameters and surface engineering of SPIONs is very important process due to the fact that the synthetic conditions determine their physicochemical characteristics, their colloidal stability, and their biocompatibility [6,7]. For diagnostic and therapeutic uses, applied magnetic systems should exhibit very small nano-size and narrow size distribution together with high saturation magnetizations [8]. Furthermore, SPIONs must show loss of magnetization after removal of the magnetic field, where they should have negligible remanence and low coercivity values after removal of magnetic field. In spite of the above mentioned magnetic advantages, there is a need to surface grafting SPIONs with a polymer for various bio-applications, where it was reported that in the absence of surface layer SPIONs are formed aggregate forms, decrease of surface activity, promoted their rapid elimination by macrophages and hence their blood half-life in circulation is strongly reduced [9,10]. In this regard, various biomolecules/biopolymers like as dextran, PVA chitosan, PEG, starch, PEI, EDAT, PVP, have been applied as SPIONs surface coat [11-22].

Moreover, the proper surface capping layer onto the SPIONs particles is desired to provide suitable biocompatibility, low cell toxicity and specific localization at the targeted cell [23,24]. SPIONs possessing appropriate physicochemistry and tailored surface properties have been extensively investigated for various applications such as magnetic resonance imaging (MRI), hyperthermia, drug delivery, bio-sensing, biochemical separations, tissue engineering, cancer therapy, and bio-analysis [25-32]. As the results of these proper characteristic of SPIONs, various clinical trials are currently applied to determine the potential of different SPIONs-based nano-systems for biomedical and pharmaceutical uses.

As a simple method for preparation of nanomaterials, cathodic electrodeposition exhibits as a facile method for the fabrication of nanomaterial due to its ability in controlling crystal phase, size and composition of products [33-44]. Up now, various techniques for the preparation of SPIONs have been reported, which include co-precipitation, solution plasma, sonolysis, electrochemical deposition, mechanochemical dispersion, arc discharge, synthesis in reverse micelles and sol–gel processes, solvothermal, spray and laser pyrolysis, thermal decomposition, flow injection synthesis, hydrothermal, and combustion synthesis [45-50]. Recently, the cathodic deposition method has been previously applied for metal ion doped SPIONs [51-56], where an improvement in the magnetic behavior of iron oxide particles has been reported. Here, we report a simple cathodic deposition platform for fabrication of dextran-coated and Zn^{2+}-doped iron oxide nanoparticles (DEX/Zn-SPIONs). The prepared SPIONs are characterized through XRD, FE-SEM, FT-IR, DSC-TGA and VSM analyses.

2. EXPERIMENTAL PROCEDURE

2.1. Electrochemical preparation of SPIONs

All chemicals were purchased from Merck Company, and used without purification. For preparation of electrolyte solution; First, 0.75 g iron(II) chloride $6H_2O$, 1.5 g iron(III) nitrate $9H_2O$, and 0.25 g zinc nitrate $6H_2O$ were dissolved in 1000cc ethanol (96%), and then 0.2 g dextran (as coating agent) was added into this electrolyte and stirred for 30 min. Electrochemical set up composed of two electrodes of copper sheets as anode and cathode, which immerged into the deposition bath. The surface areas of both copper electrodes were identical i.e. SA=10 cm%10 cm=100 cm^2. The direct current (*dc*) electroplating mode was used in the electrodeposition of SPIONs. The temperature and pH of electrolyte were 40 ^oC and 6.7, respectively. In the deposition processes, a *dc* current of 100 mA cm^{-2} was applied into the electrochemical cell for 20 min, and a black thick film was appeared on the cathode side of cell at the end of deposition time. After the deposition, the cathode sheet was removed from the electrolyte and washed with ethanol. Then the deposited film was slowly separated from the surface of copper sheet. The collected wet powder was dispersed in 100 cc ethanol (100% purity, Merck), and the solution was centrifuged at 2000 rpm for 5 min to remove the weekly bonded capping gents onto the SPIONs surfaces. In final process, the SPIONs were collected from the ethanol solution by magnet, and dried at vacuum oven (T=80^oC) for 2h. The fabricated black powder was labeled DEX/Ni-SPIONs product and used in the further analyses.

2.2. SPIONs characterization

The fabricated DEX/Zn-SPIONs powder was analyzed through field-emission scanning electron microscopy (FE-SEM, Mira 3-XMU with accelerating voltage of 100 kV) and energy dispersive diffraction X-ray analysis (EDS) to identify their surface morphology, particle size and elemental features. The crystal phase and XRD pattern of the prepared SPIONs was provided by Philips PW-1800 XRD instrument having a cobalt X-ray tube (Kα radiation=1.79Å). Thermal analysis of the fabricated SPIONs was carried out via a STA-1500 thermo-analyzer under dry air atmosphere at the temperature zone of 25-600 ^oC. The Fourier transformed infrared spectra were recorded using a Bruker Vector 22 FTIR instrument. The magnetic studies were done using vibrating sample magnetometer (Meghnatis Daghigh Kavir Co., Iran).

3. RESULTS AND DISCUSSION

Fig. 1 shows the XRD pattern of the prepared SPIONs. The recorded pattern has all typical diffraction peaks related to the magnetite phase of iron oxide, and very similar to the XRD patterns reported for undoped and metal ion doped Fe_3O_4 in literature [57,58]. The observed diffractions include (111), (220), (311), (400), (422), (511), (440), (533) and (623) which are

located at 2theta of 17.54º, 30.78 º, 35.23 º, 43.63, 54.04 º, 56.75º, 62.96 º, 71.154 º and 74.16 º, respectively. These peaks are well matched with the crystal planes of magnetite phase of iron oxide (JCPDS card No. 01-088-0315). The diffraction broadening shows the nanometer size of the fabricated SPIONs crystallites. Through the Debye–Sherrer equation (i.e. $D=K\lambda/\beta\cos\theta$) and diffraction values related to (311) peak, the average crystallite size was calculated to be 7.3 nm.

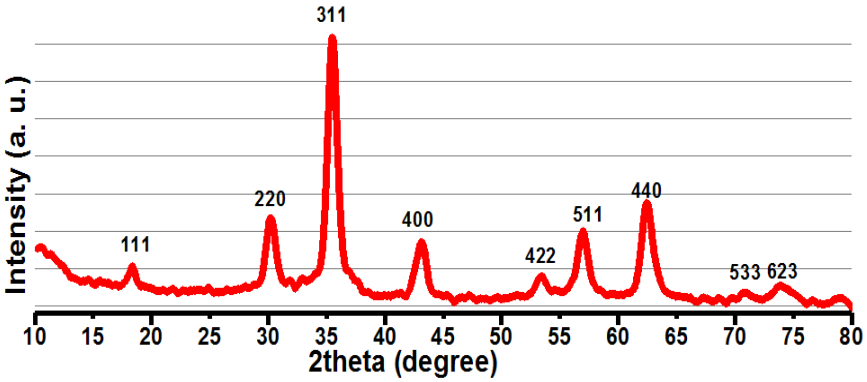

Fig. 1. XRD pattern of the fabricated SPIONs

Fig. 2 gives the FT-IR spectrum of the DEX/Zn-SPIONs sample. It is well known that IR peaks observed at the wavenumbers lower that 700cm^{-1} implicate the metal-oxygen vibrations (i.e. $\nu_{(M\text{-}O\text{-}M)}$) [58,59]. The two bands at 665 cm^{-1} and 586 cm^{-1} for SPIONs nanoparticles result from split of the ν_1 band at 570 cm^{-1} and shift to higher wavenumbers, and it was reported that these bands are related to the vibrations of the Fe-O-Fe bonds (i.e. $\delta_{(Fe\text{-}O\text{-}Fe)}$) [59].

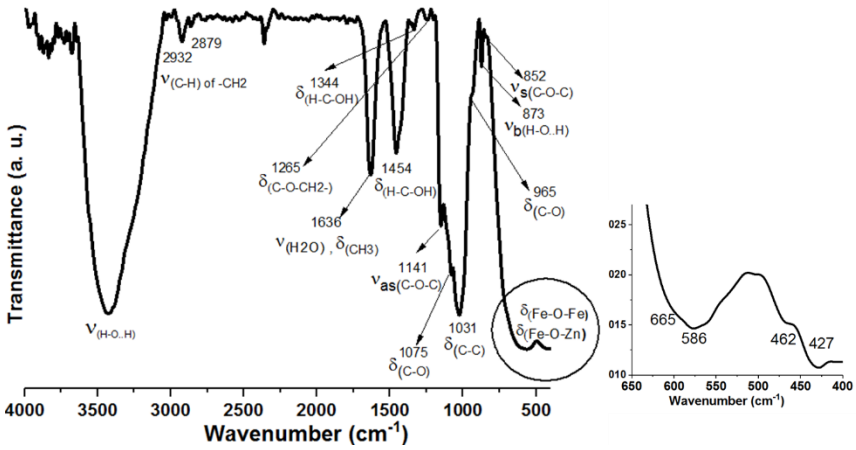

Fig. 2. IR spectrum of the fabricated SPIONs

The IR bands at 462 cm^{-1} and 427 cm^{-1} can be assigned to Fe-O-Fe/ and Fe-O-Zn bonds (i.e. $\delta_{(Fe\text{-}O\text{-}Fe)}$ and $\delta_{(Fe\text{-}O\text{-}Zn)}$) [59,60]. At high wavenumbers, there are observed various IR bands, which could be assigned to the different vibration modes of following chemical bonds [61-65];

νas(C-O-C) at 1141 cm^{-1}, νs(C-O-C) at 852 cm^{-1}, δ(CH3) at 1636 cm^{-1}, δ(C-C) at 1031 cm^{-1}, ν_b(H-O…H) at 3250-3500 cm^{-1}, ν_b(H-O…H) at 873 cm^{-1}, δ(H-C…OH) at 1454 cm^{-1}, δ(C-O..CH2) at 1265 cm^{-1}, νs(C-H) of CH_2 at at 2932 cm^{-1}, νas(C-H) of CH_2 at 2879 cm^{-1}, δ(H-C-OH) at 1344 cm^{-1} and δ(C-O) at 1075 cm^{-1}. These IR bands have all vibration modes related to the different chemical bonds presented in the chemical structure of dextran polymer, and hence it is revealed that dextran is exist in the chemical composition of the fabricated SPIONs. In fact, surface capping of SPIONs by dextran layer in proved through FT-IR results.

The measurement of thermal behavior of the fabricated SPIONs was used to prove the organic coated layer onto their particle surfaces. Fig. 3 illustrates the differential scanning calorimetry (DSC) curve and the measured loss of SPIONs weight at the temperatures of 25–600 ºC. There is a broad endothermic peak on the DSC curve (Fig. 3a) at the temperatures between 25 to175 °C, which is comes from the physical phenomena of removal of hydroxyl group, ethanol and water molecules connected or linked onto the surface of SPIONs particles [21,22]. Due to these mentioned physical process, the SPIONs powder exhibited about 2.46% weight loss on the TG curve (Fig. 3b). As the temperature increased (i.e. T>175 °C), a broad endothermic behavior between temperatures of 175 to 325 °C with peak at 265 ºC is occurred on the DSC profile of SPIONs. At the same range of temperature, TG curve showed about 9.69% weight loss (Fig. 3b). In the literature, it was reported that SPIONs capped with dextran layer exhibits a two-successive endothermic behavior at the temperatures of between 175-325 ºC with a sharp weight loss, which has been connected to the degradation of dextran layer in a two-step process [65-67]. According to these reports, the observed weight loss at T=175-325 ºC was assigned to the breakdown and removal of dextran. At final step, there is a small endothermic peak and weight loss (0.2%) at temperature of 570 ºC, which is due to the phase transition of magnetite into other phase of iron oxide. The overall weight loss of SPIONs was observed to be 12.35%. These TG data indicated the presence of dextran capped layer onto the surface of deposited iron oxide particles.

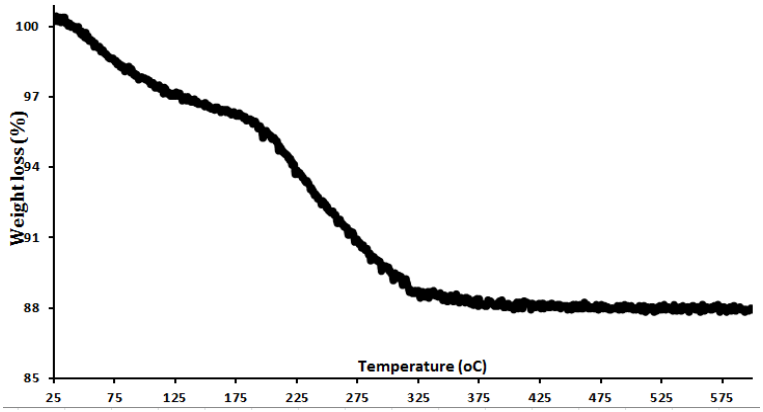

Fig. 3. DSC-TGA curves of the electrodeposited DEX/Zn-SPIONs sample

As presented in Fig. 4a, FE-SEM observations showed particles morphology with an average size of 15 nm for the electro-deposited SPIONs. Elemental data provided through EDS analysis revealed that the fabricated SPIONs powder has the iron, zinc, oxygen and carbon elements, respectively, with weight percentages of 47.05%, 10.02%, 32.07% and 10.88% in its chemical structure. From these elemental data, it is proved that (i) the prepared SPIONs have been doped with zinc cations, (ii) dextran presence is verified through carbon presence, and (iii) the magnetite phase of the prepared SPIONs is cleared from the Fe and O percentages. In final, the chemical features of particle surface capped with dextran and crystal structure doped by zinc are confirmed by EDS data.

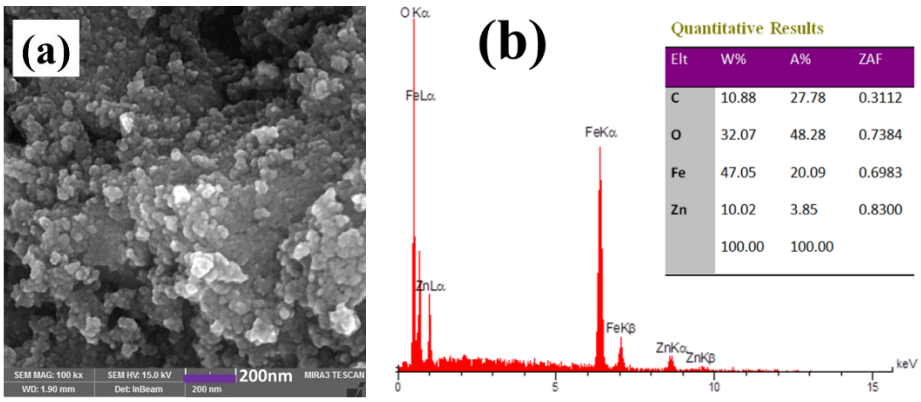

Fig. 4. (a) FE-SEM image and **(b)** EDS data of the prepared DEX/Zn-SPIONs sample

The magnetic performance of SPIONs particles in the exposure/removal of applied field was investigated using vibrating-sample magnetometer (VSM) instrument. The recorded *M-H* profile of SPIONs is shown in Fig. 5a and also the low applied zone is also magnified as presented in Fig. 5b. The form of *VSM* profile exhibited the superparamagnetic feature of the fabricated iron oxide particles, and is very similar to those reported for metal ion doped Fe_3O_4 particles in literature [68-72]. The essential magnetic parameters including saturation magnetization (*Ms*), remanence (*Mr*) and coercivity (*Hci*) values were measured to be 51.75 emu g^{-1}, 0.16 emu g^{-1} and 3.35 Oe, respectively. These data indicated that the prepared SPIONs shows relative high saturation magnetization with connecting the applied fields and also negligible *Ms* and low *Ce* values with removal of the applied field. Furthermore, the magnetic properties of our prepared SPIONs are comparable with those reported for magnetic iron oxide particles until now: e.g. *Ms*=72.96 emu/g, *Mr*=0.95 emu/g and *Ce*=14.6 Oe for naked SPIONs [52], *Ms*=45.87 for dextran capped SPIONs [61], *Mr*=0.22 emu/g and *Ce*=4.84 Oe for Mn^{2+}-doped IONs [68], *Mr*=0.15 emu/g and *Ce*=2.71Oe for Bi^{3+}-doped IONs [69], *Ms*=41.89 emu/g, *Mr*=0.12 emu/g and *Ce*=2.24 G for Sm^{3+}-doped SPIONs [70], *Ms*=52.04 emu/g, *Mr*=0.73 emu/g and *Ce* =7.56 G for Co-doped SPIONs [71] and *Ms*=46.93 emu/g, *Mr*=0.34 emu/g and *Ce*=6.25 G for Dy-SPIONs [72]. Hence, it is confirmed that the fabricated SPIONs could be

suitable magnetic system for both diagnostic and therapeutic applications like as hyperthermia, drug delivery, magnetic separation and MRI.

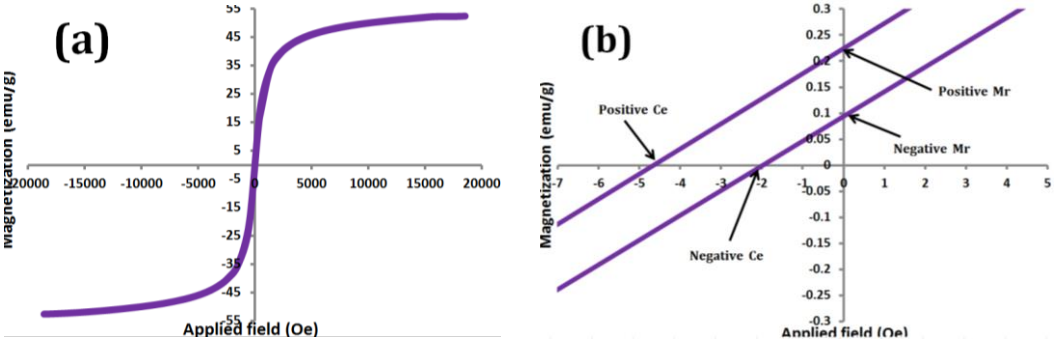

Fig. 5. Hysteresis loops for the electrodeposited the prepared DEX/Zn-SPIONs

4. CONCLUSION

In this work, dextran capped, zinc cations doped SPIONs were successfully synthesized and characterized. The preparation method of cathodic electrochemical synthesis was simply developed for fabrication of dextran grafted zinc-doped iron oxide nanoparticles. The prepared SPIONs have an average size of 15nm and uniform spherical particles. Also, SPIONs have about 10% doped Zn^{2+} ions in their crystal structure. Dextran layer with 10%wt was also capped onto the surface of Zn-SPIONs. Due to the excellent magnetic behavior (i.e. *Mr*=0.16 emu/g and *Hci*=3.35 Oe), the fabricated SPIONs was proposed for use in various imaging, targeting and therapy biomedical systems.

REFERENCES

[1] M. Mahmoudi, M. A. Sahraian, M. A. Shokrgozar, and S. Laurent, ACS Chem. Neurosci. 2 (2011) 118.

[2] L. Harivardhan Reddy, J. L. Arias, J. Nicolas, and P. Couvreur, Chem. Rev. 112 (2012) 5818.

[3] I. Karimzadeh, H. Rezagholipour Dizaji, and M. Aghazadeh, Mater. Res. Express 3 (2016) 095022.

[4] S. Laurent, D. Forge, M. Port, A. Roch, C. Robic, L. V. Elst, and R. N. Muller, Chem. Rev. 108 (2008) 2064.

[5] I. Karimzadeh, M. Aghazadeh, M. R. Ganjali, T. Dourudi, Curr. Nanosci. 13 (2017) 167.

[6] A. Kumar Guptaa, and M. Gupta, Biomater. 26 (2005) 3995.

[7] M. Faraji, Y. Yamini, and M. Rezaee, J. Iran. Chem. Soc. 7 (2010) 1.

[8] S. K. Yen, P. Padmanabhan, and S. T. Selvan, Theranostics 3 (2013) 986.

[9] B. I. Kharisov, H. V. Rasika Dias, O. V. Kharissova, A. Vazquez, Y. Pen, and I. Gomez, RSC Adv. 4 (2014) 45354.
[10] Y. Hu, S. Mignani, J. P. Majoral, M. Shen, and X. Shi, Chem. Soc. Rev. 47 (2018) 1874.
[11] M. Aghazadeh, and I. Karimzadeh, Curr. Nanosci. 14 (2018) 42.
[12] M. Aghazadeh, I. Karimzadeh, M. R. Ganjali, D. Gharailou, and P. Kolivand, Curr. Nanosci. 13 (2017) 274.
[13] I. Karimzadeh, M. Aghazadeh, M. R. Ganjali, P. Norouzi, S. Shirvani-Arani, T. Doroudi, P. H. kolivand, S. A. Marashi, and D. Gharailou, Mater. Lett. 179 (2016) 5.
[14] M. Aghazadeh, I. Karimzadeh, M. R. Ganjali, and M. M. Morad, Mater. Lett. 196 (2017) 392.
[15] I. Karimzadeh, M. Aghazadeh, M. R. Ganjali, P. Norouzi, T. Doroudi, and P. H. Kolivand, Mater. Lett. 189 (2017) 290.
[16] M. Aghazadeh, Anal. Bioanal. Electrochem. 11 (2019) 362.
[17] M. Aghazadeh, Anal. Bioanal. Electrochem. 10 (2018) 508.
[18] M. Aghazadeh, I. Karimzadeh, A. Ahmadi, M. R. Ganjali, and P. Norouzi, J. Mater. Sci.: Mater. Electron. 29 (2018) 14378.
[19] M. Aghazadeh, I. Karimzadeh, and M. R. Ganjali, Mater. Lett. 228 (2018) 137.
[20] M. Aghazadeh, I. Karimzadeh, and M. R. Ganjali, J. Mater. Sci.: Mater. Electron. 28 (2017) 13532.
[21] M. Aghazadeh, I. Karimzadeh, and M. R. Ganjali, Mater. Lett. 209 (2017) 450.
[22] M. Aghazadeh, I. Karimzadeh, and M. R. Ganjali, Curr. Nanosci. 15 (2019) 169.
[23] N. V. Srikanth Vallabani, and S. Singh, 3 Biotech 8 (2018) 279.
[24] X. Liu, S. Lu, D. Liu, L. Zhang, L. Zhang, X. Yu, and R. Liu, Brain Res. 1707 (2019) 141.
[25] S. R. Dave, and X. Gao, Wiley Interdiscip Rev. Nanomed. Nanobiotechnol. 1 (2009) 583.
[26] J. E. Rosena, L. Chana, D. B. Shieh, and F. X. Gu, Nanomedicine 8 (2012) 275.
[27] R. G. Thomas, M. J. Moon, and H. Lee, Carbohydrate Polym. 131 (2015) 439.
[28] H. Wang, C. A. Thorling, X. Liang, K. R. Bridle, J. Grice, Y. Zhu, D. H. G. Crawford, Z. P. Xu, X. Liu, and M. S. Roberts, J. Mater. Chem. B 3 (2015) 939.
[29] A. Z. Wang, V. Bagalkot, C. C. Vasilliou, F. Gu, F. Alexis, L. Zhang, M. Shaikh, and K. Yuet, ChemMedChem 3(2008) 1311.
[30] X. He, X. Shen, D. Li, Y. Liu, K. Jia, and X. Liu, ACS Appl. Bio Mater. 1 (2018) 520.
[31] H. Fakhimikabir, M. B. Tavakoli, A. Zarrabi, A. Amouheidari, and S. Rahgozar, J. Photochem. Photobiol. B 182 (2018) 71.
[32] X. Wang, J. Zhang, H. Zhang, X. Yang, and Y. Huang, J. Biomater. Sci. 29 (2018) 181.
[33] M. Aghazadeh, A. Rashidi, and M. R. Ganjali, Electron. Mater. Lett. 14 (2018) 37.
[34] M. Aghazadeh, and M. R. Ganjali, J. Mater. Sci.: Mater. Electron. 28 (2017) 11406.
[35] M. Aghazadeh, Anal. Bioanal. Electrochem. 11 (2019) 211.

[36] M. Aghazadeh, M. Ghaemi, A. N. Golikand, and A. Ahmadi, Mater. Lett. 65 (2011) 2545.
[37] M. Aghazadeh, M. G. Maragheh, M. R. Ganjali, and P. Norouzi, Inorg. Nano-Metal Chem. 27 (2017) 1085.
[38] M. Aghazadeh, A. N. Golikand, M. Ghaemi, and T. Yousefi, Mater. Lett. 65 (2011) 1466.
[39] M. Aghazadeh, M. Hosseinifard, B. Sabour, and S. Dalvand, Appl. Surf. Sci. 287 (2013) 187.
[40] M. Aghazadeh, and S. Dalvand, J. Electrochem. Soc. 161 (2014) D18.
[41] M. Aghazadeh, and M. R. Ganjali, J. Mater. Sci.: Mater. Electron. 28 (2017) 8144.
[42] M. Aghazadeh, I. Karimzadeh, A. Ahmadi, and M. R. Ganjali, J. Mater. Sci.: Mater. Electron. 29 (2018) 14567.
[43] M. Aghazadeh, T. Yousefi, and M. Ghaemi, J. Rare Earths 30 (2012) 236.
[44] M. Aghazadeh, J. Mater. Sci.: Mater. Electron. 28 (2017) 3108.
[45] D. Ling, N. Lee, and T. Hyeon, Acc. Chem. Res. 485 (2015) 1276.
[46] Z. Li, X. Li, Y. Zong, G. Tan, Y. Sun, Y. Lan, M. He, Z. Ren, and X. Zheng, Carbon 115 (2017) 493.
[47] Q. Wang, X. Zhang, L. Huang, Z. Zhang, and S. Dong, ACS Appl. Mater. Interfaces 98 (2017) 7465.
[48] X. X. Wang, T. Ma, J. C. Shu, and M. S. Cao, Chem. Eng. J. 332 (2018) 321.
[49] P. Xu, G. M. Zeng, and D. L. Huang, J. Taiwan Institute Chem. Eng. 71 (2017) 165.
[50] H. S. Jung, and H. J. Choi, J. Appl. Phys. 117 (2015) 17E708.
[51] M. Aghazadeh, M. R. Ganjali, and P. Norouzi, Mater. Res. Express 3 (2016) 055013.
[52] M. Aghazadeh, I. Karimzadeh, and M. R. Ganjali, J. Mater. Sci.: Mater. Electron. 28 (2017) 19061.
[53] M. Aghazadeh, and I. Karimzadeh, Mater. Res. Express 4 (2017) 105505.
[54] M. Aghazadeh, I. Karimzadeh, M. R. Ganjali, J. Mater. Sci.: Mater. Electron. 29 (2018) 5163.
[55] M. Aghazadeh, and M. R. Ganjali, J. Mater. Sci.: Mater. Electron. 29 (2018) 4981.
[56] M. Aghazadeh, J. Mater. Sci.: Mater. Electron. 28 (2017) 18755.
[57] G. S. Demirera, A. C. Okur, and S. Kizilel, J. Mater. Chem. B 3 (2015) 7831.
[58] M. Aghazadeh, Mater. Lett. 211(2018) 225.
[59] K. Yavari, and M. Aghazadeh, Anal. Bioanal. Electrochem. 10 (2018) 1134.
[60] M. Aghazadeh, I. Karimzadeh, M. R. Ganjali, and A. Malekinezhad, Int. J. Electrochem. Sci. 12 (2017) 8033.
[61] A. Saraswathy, S. S. Nazeer, N. Nimi, S. Arumugam, S. J. Shenoy, and R. S. Jayasree, Carbohydrate Polym. 101 (2014) 760.
[62] M. Khalkhali, S. Sadighian, K. Rostamizadeh, F. Khoeini, M. Naghibi, N. Bayat, M. Habibizadeh, and M. Hamidi, Bioimpacts 5 (2015) 141.
[63] J. L. Zhang, R. S. Srivastava, and R. D. K. Misra, Langmuir 23 (2007) 6342.

[64] S. Palchoudhury, F. Hyder, T. K. Vanderlick, and N. Geerts, Particulate Sci. Technol. 32 (2014) 224.
[65] A. K. Hauser, R. Mathias, K. W. Anderson, and Z. Hilt, J. Mater. Chem. Phys. 160 (2015) 177.
[66] A. Jurikova, K. Csach, J. Miskuf, M. Koneracka, V. Zavisova, M. Kubovcikova, and P. Kopcansky, Acta Phys. Polonica A 121(2012) 1296.
[67] O. Carp, L. Patron, D. C. Culita, P. Budrugeac, M. Feder, and L. Diamandescu, J. Thermal Anal. Calorim. 101 (2010) 181.
[68] M. Aghazadeh, I. Karimzadeh, M. R. Ganjali, and A. Behzad, J. Mater. Sci.: Mater. Electron. 28 (2017) 18121.
[69] M. Aghazadeh, I. Karimzadeh, and M. R. Ganjali, J. Electron. Mater. 47 (2018) 3026.
[70] M. Aghazadeh, and M. R. Ganjali, J. Mater. Sci. 53 (2018) 295.
[71] M. Aghazadeh, and M. R. Ganjali, J. Mater. Sci.: Mater. Electron. 29 (2018) 2291.
[72] M. Aghazadeh, and M. R. Ganjali, Ceram. Int. 44 (2018) 520.